

PROCEEDINGS REPRINT

 SPIE—The International Society for Optical Engineering

Reprinted from

Passive Materials for Optical Elements II

**14–15 July 1993
San Diego, California**



Volume 2018

120
90-10-100
073877

Radiation Damage Effects in Far Ultraviolet Filters and Substrates

Charles E. Keffer¹, Marsha R. Torr², Muamer Zukic¹,
James F. Spann², Douglas G. Torr¹, and Jongmin Kim¹¹Department of Physics
The University of Alabama in Huntsville
Optics Building, Suite 300
Huntsville, AL 35899²NASA/Marshall Space Flight Center
Space Science Laboratory
Huntsville, AL 35812

ABSTRACT

New advances in VUV thin film filter technology have been made using filter designs with multilayers of materials such as Al_2O_3 , BaF_2 , CaF_2 , HfO_2 , LaF_3 , MgF_2 , and SiO_2 . Our immediate application for these filters will be in an imaging system to be flown on a satellite where a $2 \times 9 R_E$ orbit will expose the instrument to approximately 275 krad of radiation. In view of the fact that no previous studies have been made on potential radiation damage of these materials in the thin film format, we report on such an assessment here. Transmittances and reflectances of BaF_2 , CaF_2 , HfO_2 , LaF_3 , MgF_2 , and SiO_2 thin films on MgF_2 substrates, Al_2O_3 thin films on fused silica substrates, uncoated fused silica and MgF_2 , and four multilayer filters made from these materials were measured from 120 nm to 180 nm before and after irradiation by 250 krad from a ^{60}Co gamma radiation source. No radiation-induced losses in transmittance or reflectance occurred in this wavelength range. Additional postradiation measurements from 160 nm to 300 nm indicated a 3 - 5% radiation-induced absorption near 260 nm in some of the samples with MgF_2 substrates. From these measurements it is concluded that far ultraviolet filters made from the materials tested should experience less than 5% change from exposure to up to 250 krad of high energy radiation in space applications.

1. INTRODUCTION

The Ultraviolet Imager (UVI) for the Global Geospace Science (GGG) POLAR spacecraft has been designed to acquire coherent global images of the Earth's aurora under both day and night conditions¹. The major goals of the observations are to obtain information on the temporal and spatial morphology of the aurora, as well as on the total incident energy flux and energy characteristics of the precipitating particles giving rise to the aurora. In order to achieve these goals, a fast (f/2.9) imaging camera has been developed which obtains wide field of view (8°) images through 5 specially designed FUV filters. Success in achieving the scientific goals is therefore dependent on the high performance of these filters. In addition to spectral resolution of closely spaced features (130.4 nm and 135.6 nm), the filters must also have sufficiently high throughput in order to allow detection of the relatively weak Lyman Birge Hopfield bands of N_2 , and must be capable of blocking out-of-band sunlight by a factor of 10^4 at wavelengths longer than 190 nm and isolating the OI emissions at 130.4 nm and 135.6 nm from the bright Lyman- α

emission at 121.6 nm. Attainment of these filter characteristics has required the development of a new multilayer stack named the Π multilayer.² The design approach was to obtain high filter throughput by minimizing energy losses in the filters with the Π multilayer design and by operating in a reflective, rather than transmissive, mode. Each UVI filter consists of three Π multilayer reflection filters and one transmission filter in series to achieve the necessary performance requirements. The transmission filter provides short wavelength rejection by acting as a cut-on filter while the three reflectors provide excellent long wavelength rejection. Additional blocking of sunlight beyond 190 nm is provided by a solar blind CsI photocathode in the UVI detector. A detailed description of the design and development of the UVI filters is given by Zukic, et al.³

The three year mission lifetime of the POLAR spacecraft will result in a radiation exposure to the UVI of approximately 275 krad. Radiation damage to optical materials has a long history of study in the space science and nuclear physics fields. At ultraviolet wavelengths, transmission of optical materials exposed to high energy radiation has been previously measured for a variety of bulk materials including Al_2O_3 ^{4,5}, BaF_2 ^{4,7}, CaF_2 ⁴, CsF ⁶, fused silica^{4,5,8-9}, LiF ^{4,5,10-11}, MgF_2 ^{4,5,10-11}, and several optical glass materials^{4,8}. Ultraviolet transmission has also been measured for irradiated colored glass filters and thin film interference filters⁹. Ultraviolet reflectance measurements of irradiated optical materials have been made at 121.6 nm for aluminum mirrors with MgF_2 protective coatings^{5,11}. Radiation damage effects on the materials used in these FUV filters have not been previously studied in the thin film format. In this paper we report the results of an investigation into the potential for radiation induced damage to the UVI filters by making measurements on the thin films and substrates used to fabricate the filters. Only long term radiation damage was studied since measurements were not made immediately following radiation exposure.

2. EXPERIMENTAL PROCEDURES

A set of 22 samples was selected for use in this study. These include BaF_2 , CaF_2 , HfO_2 , LaF_3 , MgF_2 , and SiO_2 single layer thin films on MgF_2 substrates (two of each), Al_2O_3 single layer thin films on fused silica substrates (two), two uncoated MgF_2 substrates, and two uncoated fused silica substrates. Two multilayer transmission filters ($\text{BaF}_2/\text{MgF}_2$ on a MgF_2 substrate) and two multilayer reflection filters ($\text{LaF}_3/\text{MgF}_2$ on a fused silica substrate) were also used. Every single layer thin film has a thickness between 8 nm and 22 nm with the exact thickness for each film material corresponding to the optimum thickness from the Π multilayer design. The filters used are 35-layer Π stacks. The complete set of samples is summarized in Table 1 and is representative of the substrates, thin films, and filters which make up the UVI filter system.

All of the test samples were prepared with 12.7 mm diameter and 2 mm thick VUV grade substrates used as received from Acton Research Corporation. BaF_3 , CaF_3 , and LaF_3 film materials were 99.9% pure from CERAC. Al_2O_3 (99.5%), MgF_2 (99.95%), and SiO_2 (99.98%) thin films were deposited with standard Balzers coating materials. HfO_2 was supplied by EM Chemicals with 99.5% purity. All depositions were completed at The University of Alabama in Huntsville Optical Astronomy Laboratory. An oil-free coating chamber with a sorption pump and cryopump was used to prevent hydrocarbon contamination of the films.

One of each type of single layer thin film, one of each type of uncoated substrate and all of the multilayer filters were mounted in an aluminum sample holder which was then sealed in an ultrahigh purity dry nitrogen purged double bag made from ultra clean radiation resistant Aclar. The samples were subsequently taken to Goddard Space Flight Center where they were exposed for 110 hours to a ^{60}Co gamma radiation source. The total dose received was 250 krad. After radiation exposure, the Aclar bag remained clear and had no visible evidence of radiation damage. The remaining single layer thin films and uncoated substrates served as control samples and received identical handling, with the exception of radiation exposure, including being sealed in an ultrahigh purity dry nitrogen purged double bag made from Aclar.

A series of reflectance and transmittance measurements was performed at the Marshall Space Flight Center Ionosphere Thermosphere Mesosphere Branch on the 22 samples described above. The preradiation measurements were performed in a hydrocarbon-free cryopumped vacuum chamber at a pressure below 10^{-5} Torr. A deuterium lamp with a MgF_2 window together with a 0.2-m vacuum monochromator provided 1 nm FWHM spectral resolution over the 120 nm to 180 nm wavelength range. Folding and collimating optics and a 6 mm diameter aperture limited the light incident on the eight position filter wheel holding the 12.7 mm diameter substrates to an area approximately 1/4th the area of the thin film. The small aperture insured that small positioning errors from rotating the filter wheel did not significantly impact the reproducibility of the measurements. A photomultiplier tube with a MgF_2 window and a semi-transparent Cs-I photocathode served as the detector for all measurements. The postradiation measurements were accomplished in a different hydrocarbon-free cryopumped vacuum chamber also at a pressure below 10^{-5} Torr. A similar deuterium lamp, 0.2-m vacuum monochromator, and aperture were used for the postradiation measurements. However, the second chamber did not have any folding and collimating optics. The same Cs-I photomultiplier tube and eight position filter wheel was used for both the pre- and postradiation measurements in the 120 nm to 180 nm wavelength range. A second set of postradiation transmission measurements was made from 160 nm to 300 nm using a Cs-Te photomultiplier tube. All reflectance measurements were performed at a 45° angle of incidence while transmittance was measured at normal incidence. Figures 1 and 2 illustrate the optical configurations for the two vacuum chambers utilized.

For the reflection measurements, two identical scans from 120 nm to 180 nm were performed on every sample both before and after the radiation exposure. A reference reflection filter was measured as a control with every reflection measurement to check the reliability and reproducibility of the data from measurement to measurement. The reference filter also insured that no systematic errors were introduced when the vacuum chamber was vented and a new set of samples was installed. Two identical transmission measurements from 120 nm to 180 nm were also performed on every sample both before and after the radiation exposure. An uncoated fused silica substrate in the incident beam served as a filter to block second order monochromator reflections for the 160 nm to 300 nm postradiation transmission measurements. Two identical scans from 160 nm to 300 nm were recorded for each sample. A reference transmission filter was measured with every transmission measurement as a check on the measurement reliability and reproducibility. The reflection and transmission reference filters also provided traceability between the two vacuum chambers used in the preradiation and postradiation measurements.

Absolute reflectance values were determined by comparing the reflected beam intensity from each filter with the reflected beam intensity from a VUV-enhanced aluminum mirror whose reflectance was calibrated using an Acton vacuum reflectometer model VRSC-100. Absolute transmittance values were determined by measuring the ratio of the transmitted beam intensity to the unattenuated beam intensity measured at an empty filter wheel position. Background signal was subtracted and signal drift was corrected using measurements before and after the filters were measured.

3. RESULTS

The primary wavelength range of interest for the UVI filters is 120 nm to 180 nm. Transmission and reflection measurements in this range were analyzed by first averaging the two scans taken for each sample. The difference, defined as the average of the postradiation measurements minus the average of the preradiation measurements, was then calculated. Figures 3 through 11 show the results for all of the thin films studied. The error bars represent one standard deviation. The preradiation measurements have a lower signal to noise ratio due to signal intensity losses from the folding and collimating optics used in the preradiation measurements but not in the postradiation measurements.

Repeated measurements of the transmission and reflection reference filters result in an estimated measurement uncertainty (σ) of 2%. Differences between the postradiation and preradiation measurements of greater than 4% are considered to be due to radiation-induced effects. Particular regard is given to those wavelengths where radiation-induced absorption bands are known to occur in the bulk materials.⁴ With this criterion as a benchmark, none of the 13 samples which each received 250 krad of radiation showed evidence of statistically significant radiation-induced changes in reflectance in the 120 nm to 180 nm wavelength range. For the transmittance measurements in the 120 nm to 180 nm range, only the MgF_2 uncoated substrate had any statistically significant changes. This sample had an apparent absorption short of 160 nm before radiation exposure which was not present after 250 krad radiation exposure.

Most of the UV optical materials that have been studied in bulk form have their strongest radiation-induced absorption bands at wavelengths longer than 180 nm.⁴ From 160 nm to 300 nm, the irradiated samples were compared with their equivalent control samples since no preradiation measurements were made in this wavelength range. Differences were calculated in the same manner as for the 120 nm to 180 nm wavelength measurements. Of the nine irradiated samples in this group, three show evidence of a small radiation-induced absorption band centered near 250 nm - 260 nm. Figures 5, 8, and 9 are for a CaF_2 film on a MgF_2 substrate, a LaF_3 film on a MgF_2 substrate, and a MgF_2 film on a MgF_2 substrate, respectively. The coincidence of the absorption with the well known 260 nm absorption band in MgF_2 ⁴ and the fact that the MgF_2 substrate is common to the three samples strongly suggests that the radiation damage is limited to the MgF_2 bulk material. The small 3 - 5% absorption seen in these three samples is near the limit of the measurement uncertainty and thus explains how four other samples with MgF_2 substrates do not show similar indications of radiation-induced absorption.

Heath and Sacher⁴ irradiated a 1.5 mm thick MgF_2 crystal with 10^{14} electrons/cm² at 1 MeV followed by 10^{14} electrons/cm² at 2 MeV. They observed 16% loss in transmittance at 120

nm and approximately 60% loss in transmittance at 260 nm. Hass and Hunter⁵ reported a 5% decrease in transmittance at 121.6 nm and approximately 20% decrease at 260 nm after exposure of their 3 mm thick MgF_2 crystal to 10^{15} electrons/cm² at 1 MeV. They attribute the smaller loss in transmittance compared with Heath and Sacher's results to a MgF_2 crystal which was probably higher in purity. Becher, et al.¹⁰ found approximately 20% decrease in MgF_2 transmittance at 260 nm from irradiation with 8×10^{12} protons/cm² at 85 MeV. Reft, et al.¹¹ measured MgF_2 transmittance losses of 10% at 121.6 nm and 14% at 180 nm from irradiation with 85 - and 600-MeV protons at a total absorbed energy of 5.7×10^{14} MeV/cm³. In the present study, the total absorbed energy in the samples with MgF_2 substrates is 5×10^{13} MeV/cm³. This is over ten times less total energy absorbed than in any of the other reports cited. The maximum 5% transmittance loss at 260 nm and no measurable change at 120 nm reported in the present study is thus in reasonable agreement with the earlier reports on radiation-induced damage in MgF_2 crystals.

Fused silica has been reported by Heath and Sacher⁴ to decrease in transmittance approximately 15% at 220 nm after irradiation with 10^{14} electrons/cm² at 1 MeV and 10^{14} electrons/cm² at 2 MeV. Hass and Hunter⁵ measured approximately 10% loss in transmittance at 220 nm after irradiation of fused silica by 10^{15} electrons/cm² at 1 MeV. Nicoletta and Eubanks⁹ used 10^{14} electrons/cm² at 1.5 MeV to irradiate fused silica and reported similar transmittance losses to Heath and Sacher. In the present study, no radiation-induced transmission losses were observed in the samples with fused silica substrates. The total absorbed energy was 3×10^{13} MeV/cm³ for these samples.

Nicoletta and Eubanks⁹ measured radiation damage in three interference filters which were shielded by 3.1 mm of fused silica and then irradiated with 2.7×10^{13} electrons/cm² of energies 0.3 MeV, 0.5 MeV, 1.0 MeV, and 1.5 MeV. Transmission losses were very small from the electron irradiation shielded by the fused silica. No changes in transmittance or reflectance have been observed in the present study which can be attributed to radiation damage in the thin films used. This is probably because only a small fraction of the energy is likely to be absorbed in the thin films and also because the radiation levels used were moderate.

4. CONCLUSION

None of the samples tested showed evidence of any major radiation-induced changes in reflectance or transmittance. Since the UVI filters are made from materials which we have tested and since they are housed within the body of the instrument where they will experience a total radiation dose of less than 20 krads, it is anticipated that they will suffer negligible loss in reflectance or transmittance during the nominal 3 year mission lifetime of the POLAR spacecraft.

5. ACKNOWLEDGEMENTS

This work was supported by NASA grant NAG8-834 and NASA contract NAS8-38145.

6. REFERENCES

1. M. R. Torr, D. G. Torr, M. Zukic, J. Spann, and R. B. Johnson, "An Ultraviolet Imager

- for the International Solar-Terrestrial Physics Mission," submitted to *Rev. Space Sci.*, Jan. 1993.
2. M. Zukic and D. G. Torr, "Multiple reflectors as narrow-band and broadband VUV filters," *Appl. Opt.* **31**, 1588-1596 (1992).
 3. M. Zukic, D. G. Torr, J. Kim, J. F. Spann, and M. R. Torr, "Far ultraviolet filters for the ISTP UV Imager," *Instrumentation for Planetary and Terrestrial Atmospheric Sensing*, SPIE Proceedings Vol. 1745, 99-107 (1992).
 4. D. F. Heath and P. A. Sacher, "Effects of a simulated high-energy space environment on the ultraviolet transmittance of optical materials between 1050 Å and 3000 Å," *Appl. Opt.* **5**, 937-943 (1966).
 5. G. Hass and W. R. Hunter, "Laboratory experiments to study surface contamination and degradation of optical coatings and materials in simulated space environments," *Appl. Opt.* **9**, 2101-2110 (1970).
 6. S. Majewski and M. K. Bently, "Gamma radiation induced damage effects in the transmission of barium fluoride and cesium fluoride fast crystal scintillators," *Nucl. Instr. and Meth.* **A260**, 373-376, (1987).
 7. M. Murashita, H. Saitoh, K. Tobimatsu, M. Chiba, T. Hirose and F. Takasaki, "Performance and radiation damage of a BaF₂ calorimeter," *Nucl. Instr. and Meth.* **A243**, 67-76 (1986).
 8. M. T. Shetter and V. J. Abreu, "Radiation effects on the transmission of various optical glasses and epoxies," *Appl. Opt.* **18**, 1132-1133 (1979).
 9. C. A. Nicoletta and A. G. Eubanks, "Effect of simulated space radiation on selected optical materials," *Appl. Opt.* **11**, 1365-1370 (1972).
 10. J. Becher, R. L. Kernell and C. S. Reft, "Proton-induced F-centers in LiF and MgF₂," *J. Phys. Chem. Solids* **44**, 759-763 (1983).
 11. C. S. Reft, J. Becher and R. L. Kernell, "Proton-induced degradation of VUV transmission of LiF and MgF₂," *Appl. Opt.* **19**, 4156-4158 (1980).
 12. L. R. Canfield, G. Hass and J. E. Waylonis, "Further studies of MgF₂-overcoated aluminum mirrors with highest reflectance in the vacuum ultraviolet," *Appl. Opt.* **5**, 45-50 (1966).

Table 1: Summary of thin films and substrates tested.

Film Type	Film Materials	Substrate
Single Layer	Al_2O_3	Fused Silica
Single Layer	BaF_2	MgF_2
Single Layer	CaF_2	MgF_2
Single Layer	HfO_2	MgF_2
Single Layer	LaF_3	MgF_2
Single Layer	MgF_2	MgF_2
Single Layer	SiO_2	MgF_2
Π Multilayer	$\text{BaF}_2/\text{MgF}_2$	MgF_2
Π Multilayer	$\text{LaF}_3/\text{MgF}_2$	Fused Silica
None	None	Fused Silica
None	None	MgF_2

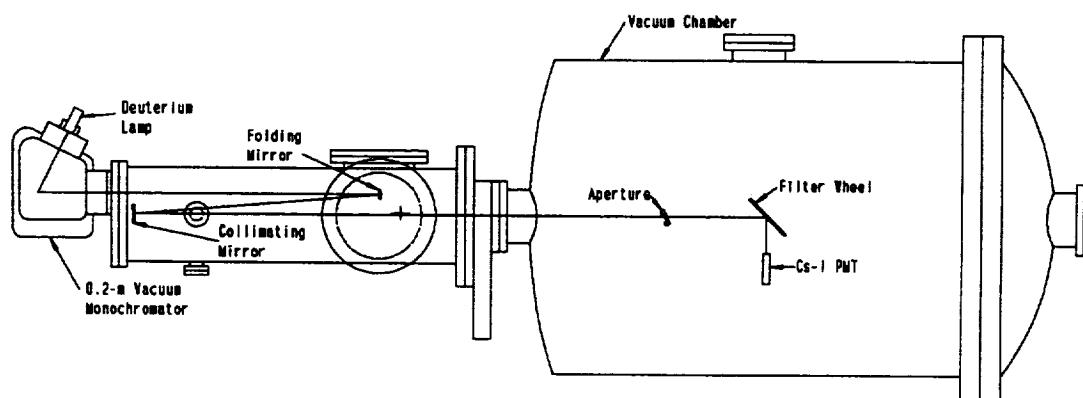


Figure 1: Vacuum chamber for preradiation measurements. Chamber is hydrocarbon free and cryogenically pumped. Optical configuration shown is for 45° reflectance measurements.

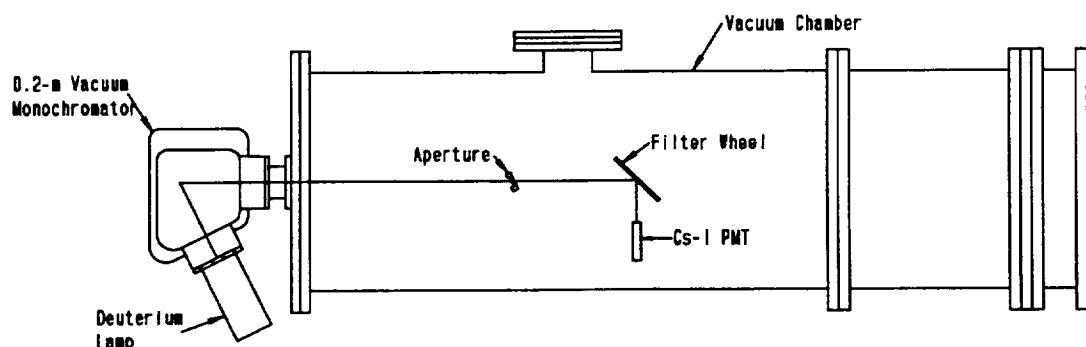


Figure 2: Vacuum chamber for postradiation measurements. Chamber is hydrocarbon free and cryogenically pumped. Optical configuration shown is for 45° reflectance measurements using a Cs-I pmt for the 120 nm to 180 nm range.

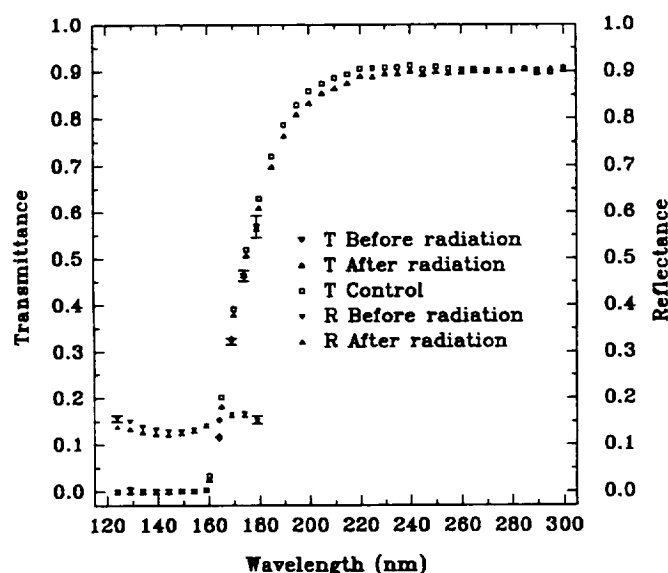


Figure 3: Reflectance and transmittance of an Al_2O_3 thin film on a fused silica substrate. Comparison is shown in the 120 nm to 180 nm range before and after radiation exposure of a single sample. In the 160 nm to 300 nm range, comparison is between the radiation exposed sample and a control sample with no radiation exposure.

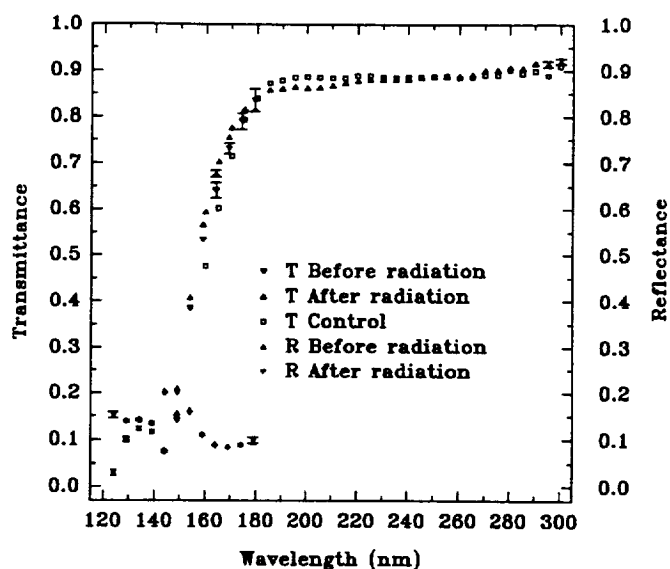


Figure 4: Reflectance and transmittance of a BaF_2 thin film on a MgF_2 substrate. Comparison is shown in the 120 nm to 180 nm range before and after radiation exposure of a single sample. In the 160 nm to 300 nm range, comparison is between the radiation exposed sample and a control sample with no radiation exposure.

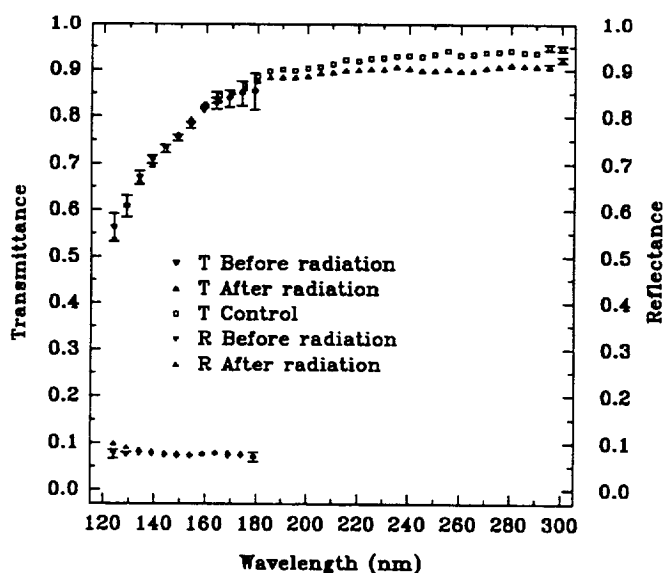


Figure 5: Reflectance and transmittance of a CaF_2 thin film on a MgF_2 substrate. Comparison is shown in the 120 nm to 180 nm range before and after radiation exposure of a single sample. In the 160 nm to 300 nm range, comparison is between the radiation exposed sample and a control sample with no radiation exposure.

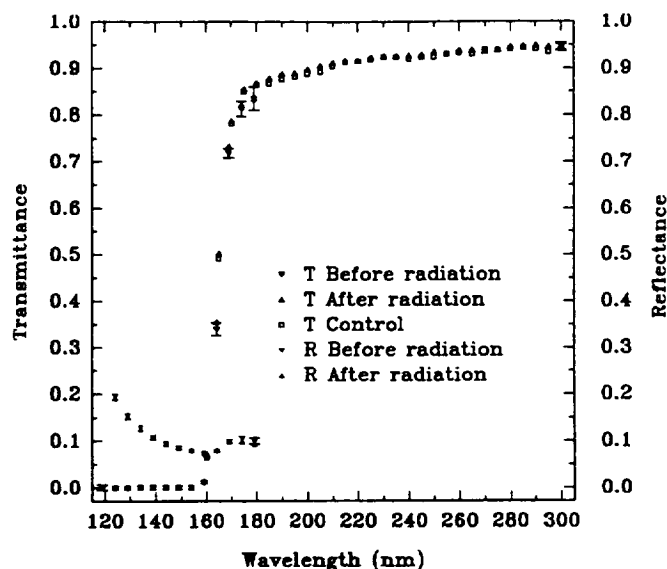


Figure 6: Reflectance and transmittance of an uncoated fused silica substrate. Comparison is shown in the 120 nm to 180 nm range before and after radiation exposure of a single sample. In the 160 nm to 300 nm range, comparison is between the radiation exposed sample and a control sample with no radiation exposure.

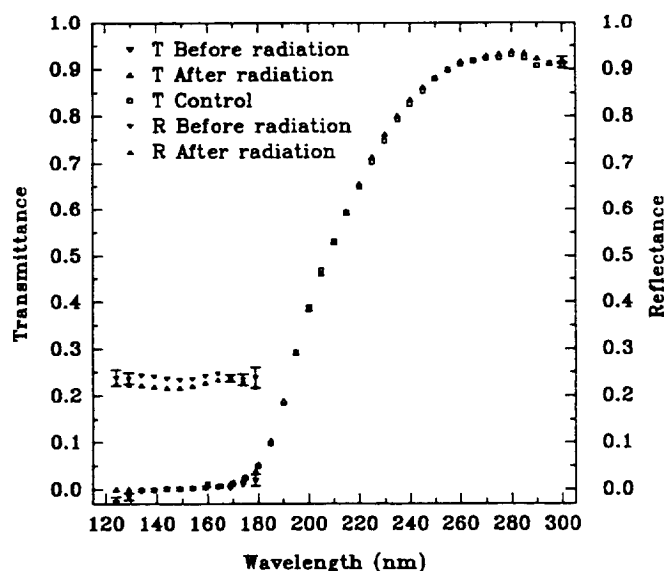


Figure 7: Reflectance and transmittance of a HfO_2 thin film on a MgF_2 substrate. Comparison is shown in the 120 nm to 180 nm range before and after radiation exposure of a single sample. In the 160 nm to 300 nm range, comparison is between the radiation exposed sample and a control sample with no radiation exposure.

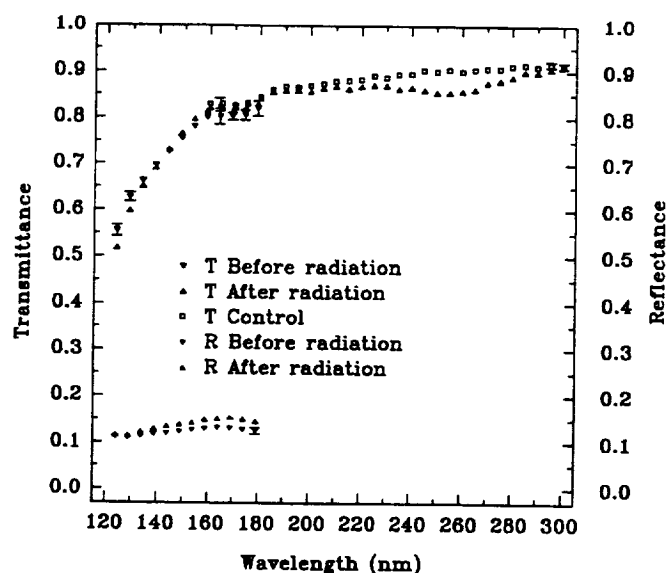


Figure 8: Reflectance and transmittance of a LaF_3 thin film on a MgF_2 substrate. Comparison is shown in the 120 nm to 180 nm range before and after radiation exposure of a single sample. In the 160 nm to 300 nm range, comparison is between the radiation exposed sample and a control sample with no radiation exposure.

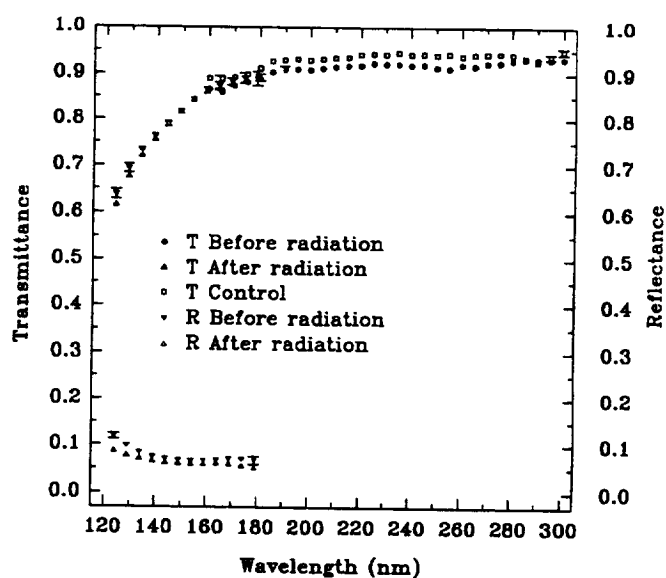


Figure 9: Reflectance and transmittance of a MgF_2 thin film on a MgF_2 substrate. Comparison is shown in the 120 nm to 180 nm range before and after radiation exposure of a single sample. In the 160 nm to 300 nm range, comparison is between the radiation exposed sample and a control sample with no radiation exposure.

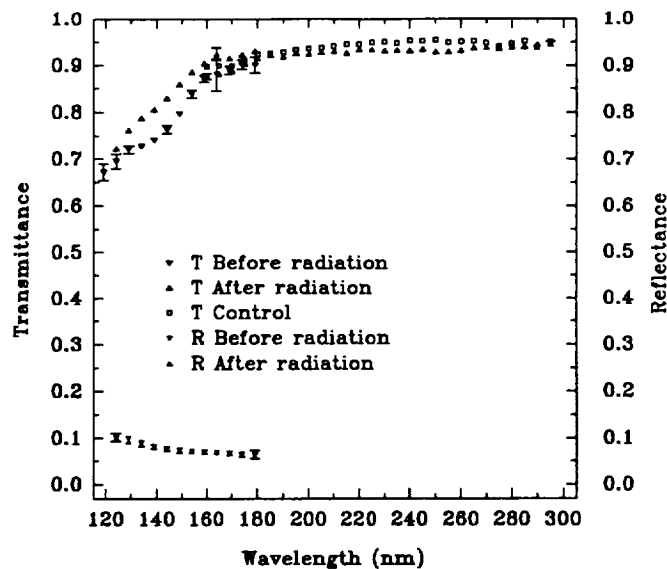


Figure 10: Reflectance and transmittance of an uncoated MgF_2 substrate. Comparison is shown in the 120 nm to 180 nm range before and after radiation exposure of a single sample. In the 160 nm to 300 nm range, comparison is between the radiation exposed sample and a control sample with no radiation exposure.

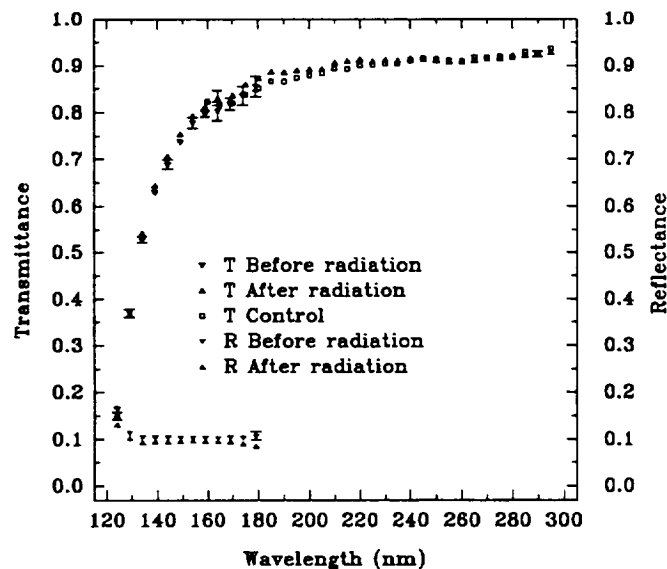


Figure 11: Reflectance and transmittance of a SiO_2 thin film on a MgF_2 substrate. Comparison is shown in the 120 nm to 180 nm range before and after radiation exposure of a single sample. In the 160 nm to 300 nm range, comparison is between the radiation exposed sample and a control sample with no radiation exposure.

